Journal of Power Sources 187 (2009) 233–237

Contents lists available at ScienceDirect

Journal of Power Sources

journal homepage: www.elsevier.com/locate/jpowsour

Short Communication

Electrochemical characteristic and discharge mechanism of a primary Li/CF_x cell

Sheng S. Zhang*, Donald Foster, Jeff Wolfenstine, Jeffrey Read

U.S. Army Research Laboratory, AMSRD-ARL-SE-DC, Adelphi, MD 20783-1197, USA

ARTICLE INFO

Article history:
Received 16 September 2008
Received in revised form 14 October 2008
Accepted 15 October 2008
Available online 5 November 2008

Keywords:
Carbon monofluoride
Graphite intercalation compound
Discharge
Impedance
Lithium battery

ABSTRACT

dc-polarization and ac-impedance techniques were used to analyze the discharge characteristic of a primary Li/CF_x cell. In most cases, impedance spectrum of a Li/CF_x cell shows a suppressed semicircle followed by a sloping straight line. The semicircle is shown to present a cell reaction resistance (R_{cr}), which reflects an ohmic resistance (mainly, ionic conductivity of the discharge product shell) and a charge-transfer process. It is shown that the overall resistance of a Li/CF_x cell is dominated by the CF_x cathode, whose resistance is further dominated by the R_{cr} that is found to be extremely sensitive to the temperature. Therefore, the low temperature performance and rate capability of a Li/CF_x cell are mainly determined by the CF_x cathode. In addition, based on the discharge curve and open circuit voltage (OCV) recovery of a Li/CF_x cell, we proposed a "core-shell" model consisting of a shrinking "CF_x core" and a growing "product shell" for the discharge process of CF_x cathode. The "product shell" plays an important role in the discharge performance of Li/CF_x cells.

Published by Elsevier B.V.

1. Introduction

Li/CF_x cells are known to have the highest theoretical capacity when compared to other primary lithium batteries such as Li/$SOCl_2$ and Li/MnO_2 batteries, and recently are being developed as soldier portable power sources [1]. The overall discharge reaction of a Li/CF_x cell is expressed as "$CF_x + xLi \rightarrow C + xLiF$". According to this reaction, the specific capacity of a CF_x cathode is associated with the content of fluorine, i.e., x value in the formula. Theoretically, a CF_x with $x = 1$ has a specific capacity of 865 mAh g^{-1}, about twice that of $SOCl_2$ currently used in primary Li/$SOCl_2$ batteries. The electronic conductivity of CF_x materials is known to decrease with an increase in the x value [2,3], for example, the material becomes entirely non-conductive as the x value approaches 1 [4]. Therefore, there is a trade-off between the specific capacity of CF_x cathode and the power capability of a Li/CF_x cell. In most non-aqueous liquid electrolytes, CF_x ($x = 1$) cathode has an open circuit potential of 3.2–3.5 V vs. Li^+/Li. However, discharge voltage of a real Li/CF_x cell ($x = 1$) is much lower than this value, showing significant polarization [5]. One reason for this high polarization is the low electronic conductivity of CF_x materials. To solve this problem, Yazami et al. [6,7] synthesized a series of subfluorinated carbon materials (CF_x, with $x < 1$) and successfully demonstrated Li/CF_x cells with much improved power capability. However, their success was made at a cost of specific capacity.

Other problems with Li/CF_x cells include: (1) voltage delay in the initial discharge period, (2) poor low temperature performance, and (3) heat generation accompanying with discharge process. These problems become much more severe when the discharge current rate is high or the temperature is low. To understand these problems, in this work we assembled a three-electrode Li/CF_x electrochemical cell and observed the individual contribution of each electrode to the polarization and impedance of the Li/CF_x cell. The discharge characteristic and discharge mechanism of the Li/CF_x cells will be discussed.

2. Experimental

CF_x ($x = 0.99$–1.08, Product # Carbofluor 1000, Advance Research Chemicals, Inc., Catoosa, OK) was used as the active cathode material. A CF_x electrode film was prepared by coating a slurry composed of 85% CF_x, 10% carbon black and 5% poly(vinylidene fluoride-co-hexafluoropropylene) (Kynar Flex™ 2801, Elf Atochem North America) in *N*-methylpyrrolidone solvent onto a Al foil. The coating was dried in an 80 °C-oven to evaporate solvent, and the resulting electrode film was either punched into small disks with a diameter of 1.27 cm^2 for test in button cells or cut into 3 × 3 (cm^2) squares for test in electrochemical cells. The shaped electrode pieces were further dried at 100 °C under vacuum for 8 h, and then transferred to a glove-box for cell assembly. In the glove-box Li/CF_x button cells were assembled for discharge tests by using a 0.5 m $LiBF_4$ solution in a 1:1 (weight) mixture of propylene carbonate (PC) and dimethoxyethane (DME) as the electrolyte and a Celgard® 3500 membrane as the separator. Meanwhile, three-electrode Li/CF_x

* Corresponding author. Tel.: +1 301 394 0981; fax: +1 301 394 0273.
E-mail address: szhang@arl.army.mil (S.S. Zhang).

0378-7753/$ – see front matter. Published by Elsevier B.V.
doi:10.1016/j.jpowsour.2008.10.076

electrochemical cells with a Li foil as the reference electrode were assembled for dc-polarization and ac-impedance tests.

Discharge and OCV recovery tests were performed on a Maccor Series 4000 cycler. In all discharge tests, the cutoff voltage was set at 1.5 V, and the C-rate was based on the theoretical specific capacity of 865 mAh g^{-1} for CF_x ($x = 1$). Connection circuitry and cell structure for dc-polarization tests of a three-electrode electrochemical cell is described elsewhere [8]. A Solartron SI 1287 Electrochemical Interface and a SI 1260 Impedance/Gain-Phase Analyzer was used to measure cell impedance by using potential-control and current-control mode, respectively. In potential-control mode, the cell was potentiostatically measured at OCV using an ac oscillation of 10 mV amplitude. In current-control mode, the cell was galvanostatically measured using an ac oscillation of 0.1 mA. A frequency range from 100 kHz to 0.01 Hz was used in both test modes, and the obtained spectra were analyzed using ZView software. All tests were performed at 20 °C unless specified otherwise. The cells were allowed to rest for 5 h to reach a stable open circuit voltage (OCV) before test.

3. Results and discussion

3.1. Discharge characteristic and mechanism

Two identical button cells were assembled to observe discharge characteristic of Li/CF_x cells. After a 5 h rest, both cells reached a stable OCV of 3.27 V and 3.33 V, respectively. These values are more than 1 V lower than the theoretical OCV, 4.57 V, calculated by Valerga et al. [9] based on thermodynamic data for the cell reaction "$Li + CF_{1.0} \rightarrow C + LiF$". This difference is ascribed to the formation of a graphite intercalation compound (GIC) intermediate with solvated lithium fluoride [10,11]. Thus, the discharge reaction of Li/CF_x cell can be described as:

Anode:

$$xLi + xS \rightarrow xLi^{+}\cdot S + xe \quad (1)$$

Cathode:

$$CF_x + xLi^{+}\cdot S + xe \rightarrow C(Li^{+}\cdot S\text{–}F^{-})_x \quad (2)$$

Overall reaction:

$$CF_x + xLi + xS \rightarrow C(Li^{+}\cdot S\text{–}F^{-})_x \quad (3)$$

where S represents one or more solvent molecules coordinated with each Li^+ ion. Upon formation, the GIC intermediate subsequently decomposes into the final discharge products, carbon and lithium fluoride, as shown below:

$$C(Li^{+}\cdot S\text{–}F^{-})_x \rightarrow C + xLiF + xS \quad (4)$$

The mechanism above has been supported by the strong effect of solvents on the cell OCV and discharge voltage [12,13]. The results indicated that the solvated Li^+ ion is intercalated into graphite fluoride layers and that the discharge voltage of a Li/CF_x cell is related to the solvation energy of Li^+ ion [12,13]. Abraham et al. further showed that the discharge of a Li/CF_x cell is accompanied by significant cathode swelling due to the formation of volumetric LiF crystals [14].

Fig. 1 shows discharge characteristic of these two identical cells. It can be seen from Fig. 1a that the voltage of both cells shows a small and current-related delay in the beginning of discharge, and then the voltage slowly recovers to the normal voltage (2.50–2.55 V) until the discharge ends. The cells deliver about 90% of theoretical capacity, however, their voltages are much lower than their OCV. This is due to the low electronic conductivity of CF_x cathode and to the slow diffusion of solvated lithium ions in the GIC intermediate layer [15]. The initial voltage delay is due to the low conductivity of fresh CF_x material, which is known to have an electrical resistivity of $\sim 10^{11}$ Ω cm [4]. The subsequent voltage recovery is due to the formation of conductive carbon as shown in Eq. (4). Very sharp differential capacity peak (see Fig. 1b) suggests that the discharge of Li/CF_x cells be carried out through a two-phase transition between CF_x phase and GIC intermediate phase. Fig. 1c shows that the recovery of cell OCV from the fully discharged state is very slow. It takes about 60 h to reach a stable voltage (~3.2 V), which is close to the real OCV of the final discharging products and is comparable with the OCV of most carbon materials. Since the discharge voltage is very flat (Fig. 1a), which does not increase with a decrease in the averaged x value, we may further consider that the Li/CF_x cell is discharged through a "core-shell" model, as illustrated in Fig. 2. It is shown that the CF_x phase is constantly remained in the core and it

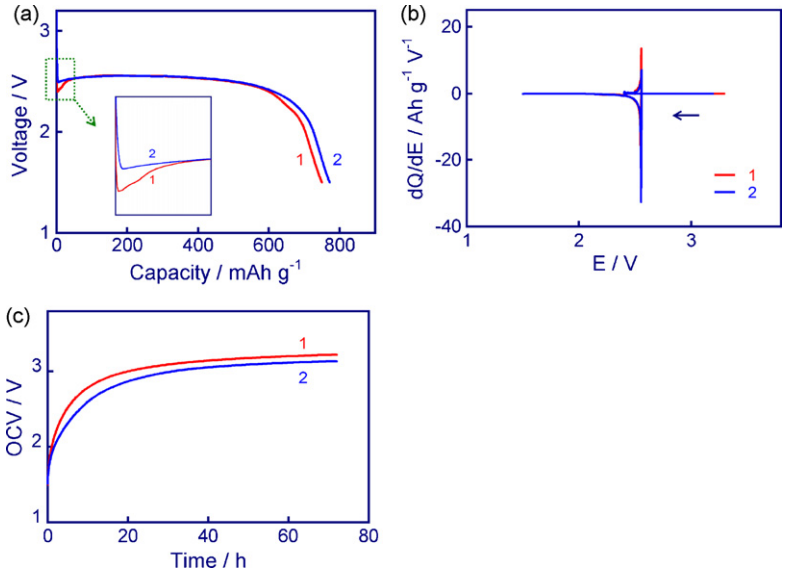

Fig. 1. Discharge characteristic of two identical Li/CF_x button cells. (a) discharge curves at $C/20$ (1) and $C/30$ (2), respectively, (b) differential capacity plots, and (c) OCV recovery curves.

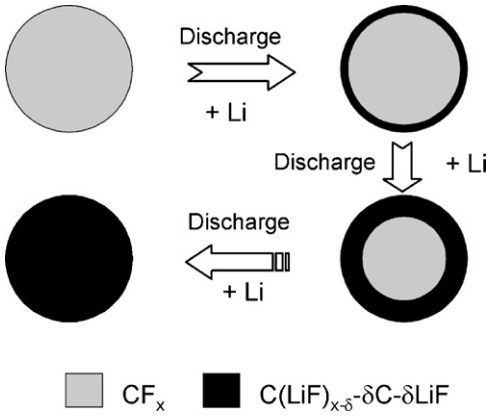

Fig. 2. Schematic illustration of a "core-shell" model for the discharge of a Li/CF_x cell.

shrinks with discharge progress until completely consumed, while the product shell consisting of GIC intermediate, carbon and lithium fluoride grows with depth of discharge (DOD). Meanwhile, the discharge process is accompanied by significant cathode swelling due to an increase in the volume of the final products. Before the complete decomposition of GIC intermediate, the composition of the product shell is varied with the progress of Eq. (4). The outer product shell plays an important role in the cell performance such as discharge polarization and heat generation.

Fig. 3 compares the OCV recovery of a Li/CF_x cell in the first 5 h from various DOD. Significant difference in the OCV recovery is observed, especially in the initial periods. That is, the rate of OCV recovery is decreased with the increase of DOD. Since the recovery of OCV relates to a process of Li^+ ion diffusion in the electrode and electrolyte [16], in the present case the recovery of OCV reflects the diffusion of Li^+ ions in the product shell and its resulting self-discharge of the double layer capacitance of the high surface carbon formed during the discharge of Li/CF_x cell [17]. The observed decrease in the OCV recovery rate with DOD is consistent with the fact that the thickness of product shell grows and the volume of CF_x cathode swells, both of which increase diffusion path of Li^+ ion.

3.2. dc-polarization

Fig. 4 exhibits the correlation of cell polarization and DOD. A "quasi-OCV" was recorded after a 5 h rest at each 5% DOD increment, and the difference between "quasi –OCV" and discharge voltage was defined as the cell polarization. As shown in Fig. 4, the cell has 0.94 V polarization in the beginning of discharge, and the polarization gradually decreases with the increase in DOD. This trend is in consistence with the fact that conductive carbon is progressively

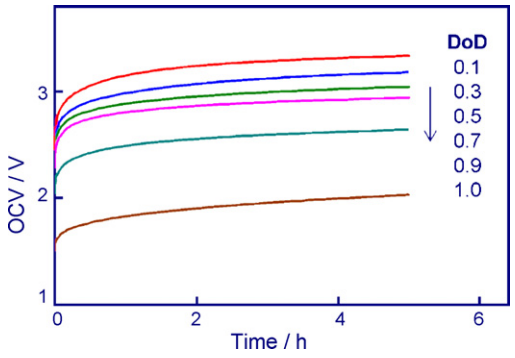

Fig. 3. OCV recovery curves of a Li/CF_x cell at different DODs.

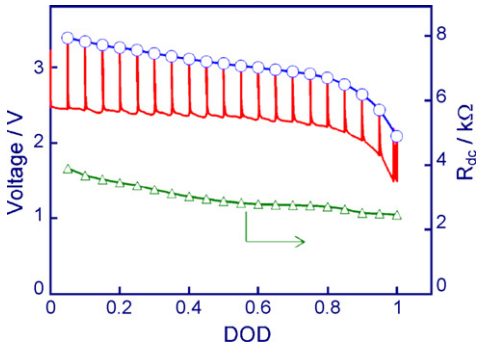

Fig. 4. Change of the OCV (circles) and dc-resistance (R_{dc}, triangles) with DOD for a Li/CF_x cell. The curve with spikes is a discharge voltage at *C*/20 and the spikes show voltage rise during a 5 h rest for the measurement of cell OCV.

formed with the discharge progress. Based on polarization voltage and discharge current, dc-resistances are calculated and plotted as a function of DOD in Fig. 4, showing that the dc-resistance of a Li/CF_x cell is decreased with DOD.

To distinguish the role of Li anode and CF_x cathode in the polarization of Li/CF_x cells, we used a three-electrode Li/CF_x electrochemical cell to monitor the potentials of each electrode and the voltage of the Li/CF_x cell. Fig. 5 records changes in the electrode potential and cell voltage when the discharge current was increased from 0.4 to 2.0 mA followed by remaining at 2.0 mA for 20 min, and then was lowered back to 0.4 mA. During this course, the change in the potential of Li anode was negligible, while that of CF_x cathode was significant and it dominated the polarization of whole Li/CF_x cell.

3.3. ac-impedance

Fig. 6 compares impedance spectra of each electrode and of the Li/CF_x cell, which were recorded from a three-electrode Li/CF_x electrochemical cell. Again, the CF_x cathode dominates the impedance of whole cell, and its impedance spectrum is very similar with that of the whole cell. Impedance spectrum of the CF_x cathode shows a suppressed semicircle at high frequencies, followed by a sloping straight line at low frequencies (see Fig. 6). The intercept at high frequency represents an ohmic resistance (R_b) contributed by the current collector, electrode, separator and electrolyte. The suppressed semicircle is rather complicated. In reference with the impedance spectra of other lithium batteries [18,19], we consider that this semicircle reflects a combined effect of the contact

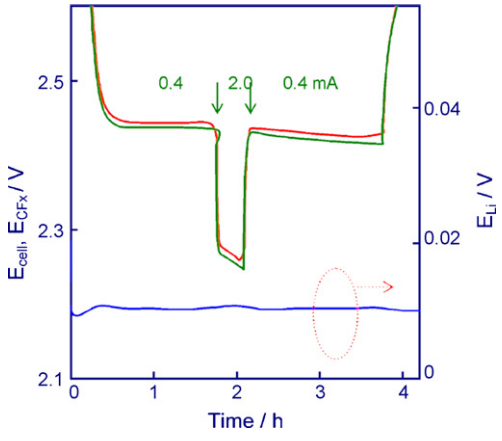

Fig. 5. Comparison for the polarization of Li anode, CF_x cathode and Li/CF_x cell during a change in the discharge current.

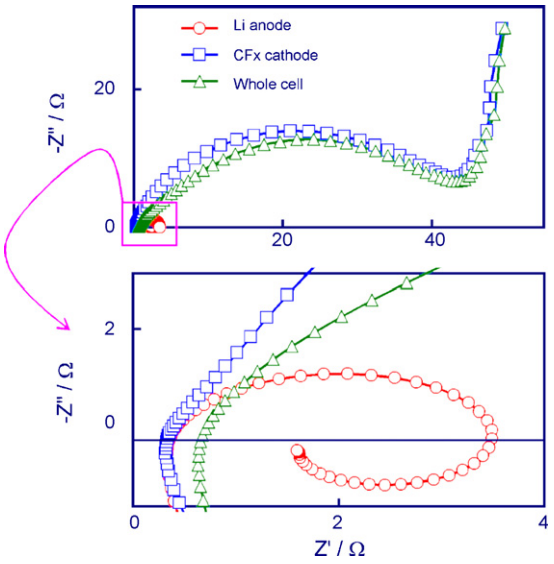

Fig. 6. Impedance spectra of Li anode, CF_x cathode and Li/CF_x cell, which were measured from a three-electrode Li/CF_x electrochemical cell at 30% DOD.

resistance between conductive particles, product shell resistance, and charge-transfer resistance. For the convenience of discussion, we call the overall resistance contributing to the suppressed semicircle as cell reaction resistance (R_{cr}). The impedance spectrum of the Li anode seems unusual, its low frequency region that corresponds to a charge-transfer process presents an inductive semicircle, instead of an impedance semicircle as observed elsewhere [20]. The reason for this inductive semicircle could be attributed to the feature of Li^+ ion semi-block of CF_x counter electrode. That is, the CF_x electrode accepts Li^+ ions through Eq. (2) in one polarity, while blocks Li^+ ions in the opposite polarity. In accordance with the CF_x cathode, we call the sum of passivation layer resistance and charge-transfer resistance in the Li anode as the R_{cr}, and the sum of R_b and R_{cr} as the cell resistance (R_{cell}). It can be seen from Fig. 6 (bottom) that the Li anode and CF_x cathode have very similar R_b, each of which occupies about the half of the cell's ohmic resistance. However, the R_{cr} of the CF_x cathode is predominantly larger than that of Li anode (see top one in Fig. 6). This observance is in good agreement with the result of the dc-polarization.

The resistances of Li anode, CF_x cathode and Li/CF_x cell at different temperatures are compared in Fig. 7. It is shown that the effect of temperature on the resistance of a Li anode is very little, as compared with those on the resistances of the CF_x cathode and Li/CF_x cell. Again, we show that the CF_x cathode dominates the overall resistance of the Li/CF_x cell. The resistance of the CF_x cathode rapidly rises as the temperature falls below −20 °C. The above results reveal that the low temperature performance and rate capability of a Li/CF_x cell is mainly determined by the CF_x cathode, instead of the Li anode. Therefore, the future improvement on the discharge performance of Li/CF_x cells should be focused on the CF_x cathode, including CF_x material, CF_x electrode processing, and electrolytic solvents that affect the formation of GIC intermediate.

Fig. 8 displays the correlation of R_b and R_{cr} with DOD for a Li/CF_x cell. The change of the R_b with DOD is not as obvious as that of R_{cr}. A gradual decrease in the R_b is observed only in the DOD range from 0% to 30%, further increase in DOD does not change R_b. The correlation between R_{cr} and DOD is rather complicated. The R_{cr} shows a sharp decrease in the first 10% DOD. This corresponds to the formation of conductive carbon, which is believed to facilitate cell reaction by enhancing electronic contact between CF_x particles and conducting agent. Beyond 10% DOD, the R_{cr} is affected by

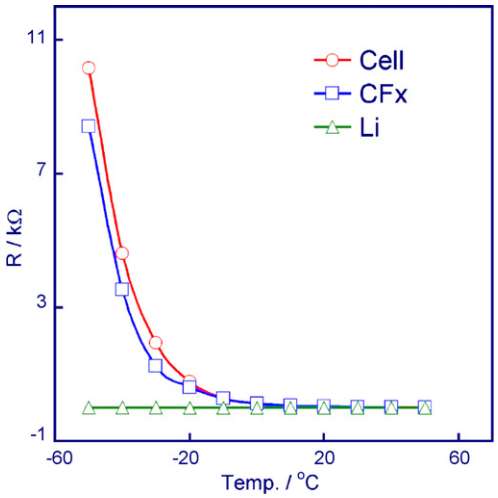

Fig. 7. Temperature dependence of the resistance of Li anode, CF_x cathode and Li/CF_x cell, which were measured from a three-electrode Li/CF_x electrochemical cell at 20% DOD.

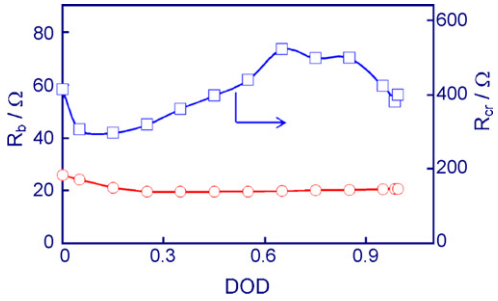

Fig. 8. Change of bulk resistance (R_b) and cell reaction resistance (R_{cr}) with DOD for a Li/CF_x button cell at 20 °C.

two opposite factors: (1) progressive formation of the conductive carbon, which increases electronic conductivity of the CF_x cathode, and (2) increased growth of the product shell, which suppresses the diffusion of Li^+ ions from the electrolyte to CF_x lattice spaces. As a result of the interaction of these two opposite factors, the R_{cr} present maxima between 65% and 85% DOD.

Fig. 9 shows the effect of discharge current on the R_{cr}, in which the impedance spectra were measured by applying a constant discharge current. The semicircle reflecting R_{cr} is obviously shrunk with an increase in the discharge current. This means that the R_{cr} is decreased with the increase of discharge current. Interest-

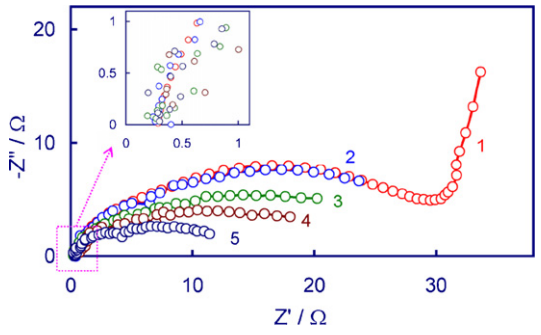

Fig. 9. The effect of discharge current on cell impedance for a Li/CF_x cell, in which the cell had a theoretical capacity of 38 mAh and the measurement started from 25% DOD in an order of the discharge current: (1) 0 mA, (2) 0.2 mA, (3) 1.0 mA, (4) 3.0 mA, and (5) 10 mA.

ingly, the semicircle splits into two different semicircles as the current increases to 10 mA (see curve 5). In reference with previous work on lithium batteries [18,19], the semicircle at high frequencies responds to an ohmic process (ionic conductivity) of the product shell, while the one at low frequencies relates to a charge-transfer process that takes place on the electrode–electrolyte interface. The size of semicircles indicates that the charge-transfer process is more resistive than the ohmic process.

4. Conclusions

Based on the discharge and OCV recovery characteristics of Li/CF_x cells, we conclude that the discharge of CF_x cathode takes place between CF_x phase and GIC intermediate phase through a "shrinking core" model consisting of a CF_x core and a product shell. The product shell is composed of GIC intermediate, carbon and lithium fluoride. The product shell grows with the discharge process, and its composition varies with the decomposition of GIC intermediate. Both dc-polarization and ac-impedance results show that the overall impedance of a Li/CF_x cell is predominated by the resistance of CF_x cathode, and that the low temperature performance and rate capability of a Li/CF_x cell are determined by CF_x cathode. The results of this work suggest that future improvement on the performance of Li/CF_x cells should be focused on the CF_x cathode, including CF_x material and electrode processing, and on the electrolytic solvents that affect the formation of GIC intermediate.

References

[1] A. Suszko, R. Thompson, D. Stevens, Workshop on Carbon Fluorides for Lithium Batteries, Pasadena, CA, February 26, 2006.
[2] T. Nakajima, R. Hagiwara, K. Moriya, N. Watanabe, J. Electrochem. Soc. 133 (1986) 1761.
[3] T. Nakajima, A. Mabuchi, R. Hagiwara, N. Watanabe, J. Electrochem. Soc. 135 (1988) 273.
[4] Advance Research Chemicals, Inc., Carbonfluor product brochure.
[5] D. Linden, T.B. Reddy (Eds.), Handbook of Batteries, third ed., McGraw-Hill, 2002 (Chapter 14.9).
[6] P. Lam, R. Yazami, J. Power Sources 153 (2006) 354.
[7] R. Yazami, A. Hamwi, K. Guerin, Y. Ozawa, M. Dubois, J. Giraudet, F. Masin, Electrochem. Commun. 9 (2007) 1850.
[8] S.S. Zhang, K. Xu, T.R. Jow, J. Power Sources 160 (2006) 1349.
[9] A.J. Valerga, R.B. Badachhape, G.D. Parks, P. Kamarchick, J.L. Wood, J.L. Margrave, Final Report for Contact # DAAB 07-73-C-0056 (ECOM), Rice University, Austin, TX, 1974.
[10] M.S. Whittingham, J. Electrochem. Soc. 122 (1975) 526.
[11] N. Watanabe, Solid State Ionics 1 (1980) 87.
[12] N. Watanabe, R. Hagiwara, T. Nakajima, H. Touhara, K. Ueno, Electrochim. Acta 27 (1982) 1615.
[13] J. Giraudet, C. Delabarre, K. Guerin, M. Dubois, F. Masin, A. Hamwi, J. Power Sources 158 (2006) 1365.
[14] K.M. Abraham, D.M. Pasquariello, Primary and secondary lithium batteries, in: K.M. Abraham, M. Salomon (Eds.), The Electrochemical Society Proceedings, 1991, PV91-3.
[15] R. Hagiwara, T. Nakajima, N. Watanabe, J. Electrochem. Soc. 135 (1988) 2128.
[16] Q. Wang, H. Li, X. Huang, L. Chen, J. Electrochem. Soc. 148 (2001) A737.
[17] S. Davis, E.S. Takeuchi, W. Tiedemann, J. Newman, J. Electrochem. Soc. 154 (2007) A477.
[18] S.S. Zhang, K. Xu, T.R. Jow, J. Electrochem. Soc. 149 (2002) A1521.
[19] S.S. Zhang, K. Xu, T.R. Jow, Electrochem. Solid State Lett. 5 (2002) A92.
[20] S.S. Zhang, M.H. Ervin, K. Xu, T.R. Jow, Electrochim. Acta 49 (2004) 3339.